Journal of Alloys and Compounds 500 (2010) L26–L30

Contents lists available at ScienceDirect

Journal of Alloys and Compounds

journal homepage: www.elsevier.com/locate/jallcom

Letter

Texture and anisotropy of a hot rolled Ti–16Nb alloy

S. Banumathy[a], R.K. Mandal[b], A.K. Singh[a,*]

[a] Defence Metallurgical Research Laboratory, Kanchanbagh, Hyderabad 500058, India
[b] Centre of Advanced Studies, Department of Metallurgical Engineering, Banaras Hindu University, Varanasi 221005, India

ARTICLE INFO

Article history:
Received 18 December 2009
Received in revised form 30 March 2010
Accepted 1 April 2010

Keywords:
Ti–Nb alloy
Hot rolling
Texture
Anisotropy

ABSTRACT

This work deals with the texture, microstructure and anisotropy in mechanical behaviors of a hot rolled Ti–16Nb alloy. It exhibits low in-plane anisotropy in terms of yield strength, ultimate tensile strength and yield locus. Such an isotropy seems to arise owing to fibers present in (0 0 2), (0 2 0) and (1 1 1) pole figures. The work hardening behavior of the alloy reveals the presence of two slopes indicating that two different mechanisms are operative during tensile test. The work hardening curves follow modified Ludwik equation.

1. Introduction

Titanium and its alloys, owing to their attractive properties find a wide range of applications in aerospace, automotive, chemical and biomedical industries. Many of the components for such applications are produced by thermomechanical processing. As a consequence of this, typical textures are developed at different stages of processing. The evolution of textures has been explained by a combination of active slip systems as well as by the presence of microstructural anisotropies. The texture and anisotropy in mechanical properties of titanium and its alloys have been discussed in Refs. [1,2].

Titanium and its alloys are by and large processed by hot rolling in order to break the cast structure and to produce the homogeneous microstructure. Hot rolling results in strong texture due to low symmetry of the α (closed packed hexagonal (cph)) phase, which in turn induces pronounced anisotropy in mechanical properties. Such an anisotropy of titanium alloys consisting of α and α + β phases has been studied by several investigators [3–9]. However, similar studies are lacking in alloys comprising α″ (orthorhombic) and β phases. The α″ phase has been observed during thermomechanical processing of several commercial α + β and β titanium alloys [10–12]. Hence, it is necessary to investigate the relation among texture, microstructure and mechanical behavior of this phase.

The Ti–Nb binary alloys are widely used as superconducting and aerospace applications [13]. Such alloys containing non-toxic elements have also been considered as potential materials for biomedical applications. These alloys have attracted extensive attention of the researchers due to low elastic modulus, shape memory characteristics as well as for super plasticity [14–17]. Keeping the importance of such class of alloys in view, this investigation has been taken up. This paper reports texture, microstructure, and anisotropy in mechanical properties of a hot rolled Ti–16Nb alloy. It is to be noted that the hot rolled Ti–16Nb alloy consists of α″ and small amount of β phases. The yield locus of the hot rolled specimen has been determined using Knoop hardness method [18,19]. This paper makes an attempt to establish correlation among texture, mechanical properties and work hardening behavior of the hot rolled Ti–16Nb alloy.

2. Experimental

Six hundred gram of pancake of the alloy Ti–16Nb was prepared by non-consumable arc melting. The charge was melted repeatedly for six times to ensure chemical homogeneity. The analyzed chemistry was found to be Ti 83.6 (atom %), Nb 16.4 (atom %), O 1010 ppm, N 63 ppm and H 26 ppm. The as-cast material was unidirectionally hot rolled at 800 °C to attain 80% reduction. The specimen was deformed 5% in each pass and rolling reduction was kept strictly unidirectional. After each pass, the sample was kept back into the furnace to retain the rolling temperature. Microstructural characterization of hot rolled specimens was done in three sample planes i.e. normal direction (ND), transverse direction (TD) and rolling direction (RD). The specimens were prepared following standard metallographic technique used for titanium and its alloys. All the samples were etched with Kroll's reagent. The X-ray diffraction (XRD) studies of bulk samples were carried out using a Philips 3020 diffractometer with CuKα radiation.

The texture was measured on sheet specimen of the hot rolled material of 25 mm × 15 mm size. The 'inel G3000' texture goniometer coupled with curved position sensitive detector with CuKα radiation was employed for texture investigation

* Corresponding author at: Defence Metallurgical Research Laboratory, Kanchanbagh, Hyderabad 500058, India. Tel.: +91 40 24586488; fax: +91 40 24340683.
E-mail address: singh_ashok3@rediffmail.com (A.K. Singh).

0925-8388/$ – see front matter © 2010 Elsevier B.V. All rights reserved.
doi:10.1016/j.jallcom.2010.04.022

Table 1
Mechanical properties of hot rolled Ti–16Nb alloy.

Sample direction	0.02% YS (MPa)	UTS (MPa)	Elongation (%)	YS (MPa) by yield locus	
				Tension[a]	Compression[a]
Longitudinal (L)	580 ± 9	734 ± 9	12.6 ± 1.5	3065	2975
45°	579 ± 12	722 ± 11	18.6 ± 1.5	–	–
Transverse (T)	577 ± 10	727 ± 14	15.0 ± 0.9	3077	3127

[a] The value of YS and UTS obtained from yield locus plot (Fig. 6).

using Schultz back reflection technique [20]. For the orthorhombic phase, ten incomplete pole figures [(0 2 0), (0 0 2), (1 1 1), (0 2 1), (1 1 2), (0 2 2), (1 3 0), (1 1 3), (0 2 3) and (2 2 1)] up to ($\chi = 80^\circ$) were recorded. These pole figures were corrected for defocusing and absorption using a powder sample of Ti–16Nb alloy consisting of orthorhombic (α'') phase. From the pole figure data, the complete orientation distribution function (ODF) has been calculated with triclinic sample symmetry [21]. The results are presented as ODF plot of constant φ_2 section (120°) with iso-intensity contours in the Euler space defined by the Euler angles φ_1, Φ, φ_2 and (0 0 2), (0 2 0) and (1 1 1) pole figures. The tensile properties of the alloy were evaluated on a screw driven Instron 1185 testing machine in three-test directions namely, the longitudinal (L), 45° (specimen axis at 45° to the rolling direction) and transverse (T). The sample dimension is shown in Fig. 1. Three specimens were tested in each condition and average values of 0.2% yield strength (YS), ultimate tensile strength (UTS) and elongation are reported in Table 1. Tensile fracture surfaces were observed under scanning electron microscope (SEM-Leo 440i) in order to understand the mode of failure. A MATSUZAWA (MMT-X7) Knoop hardness tester with 100 g load was used for the determination of yield locus [18,19].

3. Results and discussion

The 3D-Optical microstructure of the hot rolled Ti–16Nb alloy is shown in Fig. 2 which reveals the presence of both the unrecrystallised and recrystallised prior β grains oriented along rolling direction. The volume fraction of recrystallised grains is considerably large. It is well known that hot rolling consists of both deformation and dynamic recrystallisation. The presence of aforesaid two types of grains in the microstructure can therefore be attributed to deformation and dynamic recrystallisation during hot rolling. The prior β grains consist of very fine distribution of constituent phases. The XRD studies confirm the presence of α'' and β phases (Fig. 3). The relative intensities of peaks corresponding to these phases indicate that the specimen consists of mainly α'' phase with small amount of β. The texture of hot rolled specimen is shown in Fig. 4. The (0 0 2) and (0 2 0) pole figures display inhomogeneous fibers 45° and 35° away, respectively from the centre while the (1 1 1) pole figure exhibits maximum intensity at the centre. The maximum intensity in (0 0 2) pole figure lies at ND-RD axis and a weak basal component ($\chi = 0.0^\circ$ and $\phi = 0.0^\circ$ with 1.7 times random) is also seen at the centre. The pole figures are asymmetric indicating the presence of triclinic sample symmetry. The main texture component in ODF lies at $\varphi_1 = 60.0^\circ$, $\Phi = 60.0^\circ$, $\varphi_2 = 120.0^\circ$ with $f(g) = 21.2$ times random. Only $\varphi_2 = 120.0^\circ$ section of ODF is shown in Fig. 4 since it consists of the main texture component. A weak inhomogeneous [0 0 1]||ND fiber which corresponds to basal component is also seen in all the φ_2 sections at $\Phi = 0^\circ$. Another inhomogeneous fiber with high intensity, consisting of the main component is located in $\varphi_2 = 120.0^\circ$ section around $\Phi = 60^\circ$ with nearly 10° spread (Fig. 4).

The engineering stress–strain curves of the hot rolled alloy in all the three directions show that the flow stress continuously

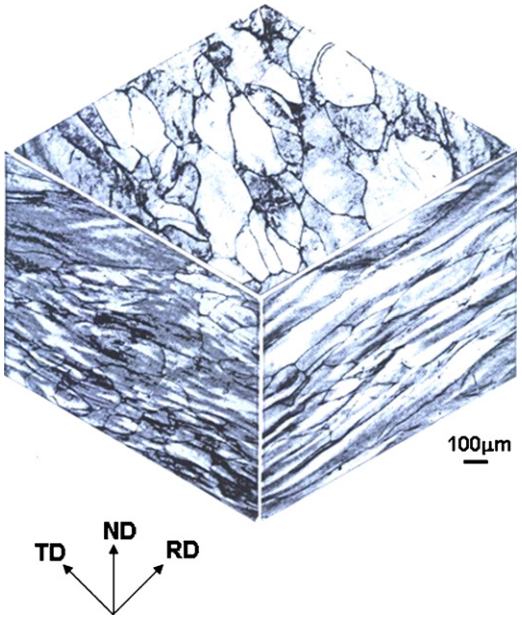

Fig. 2. 3D Optical microstructure of the hot rolled Ti–16Nb alloy.

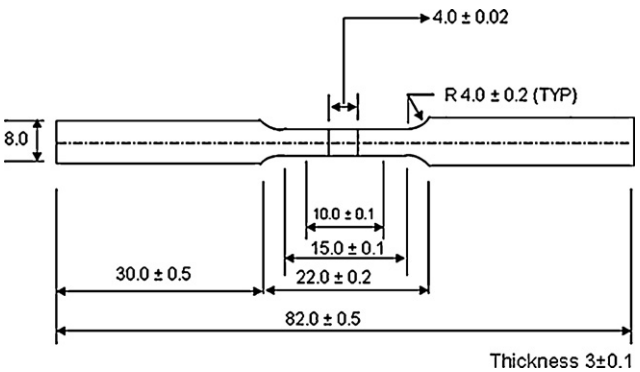

Fig. 1. A schematic diagram of tensile specimens showing the sample dimension (all are in mm).

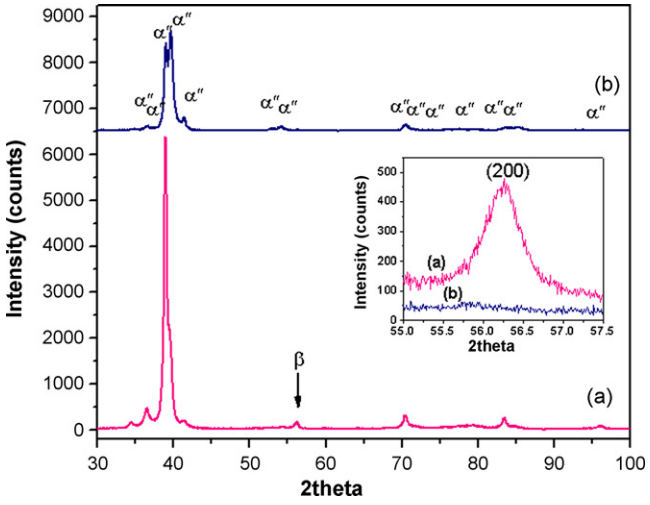

Fig. 3. The XRD patterns of the hot rolled Ti–16Nb alloy (a) before tensile test showing α'' and β phases and (b) after tensile test having only α'' phase peaks. The (2 0 0) peak of the β phase (a) before and (b) after tensile test is shown as inset.

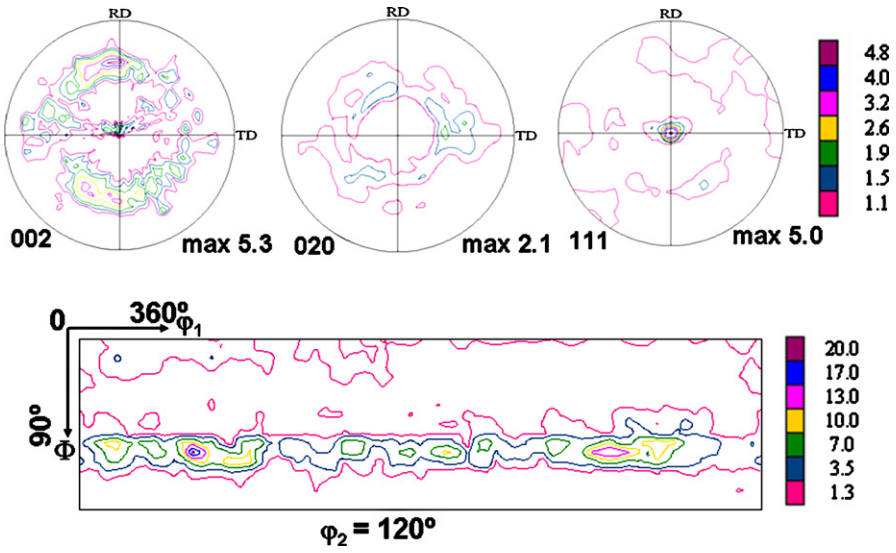

Fig. 4. Texture of the hot rolled Ti–16Nb alloy.

increases till the point of fracture (Fig. 5a). The corresponding true stress–true strain curves exhibit positive slope indicating work hardening (Fig. 5b). These curves in three specimen directions are nearly identical. The composition of the present alloy is similar to β type titanium alloys. A class of β also displays low or negative work hardening rate [22]. The mechanical properties of the hot rolled Ti–16Nb alloy along three directions namely the longitudinal (L), 45° and transverse (T) are summarized in Table 1. Fracture surfaces of the tensile specimens are similar in all three-test directions and exhibit classical ductile features. The hot rolled alloy exhibits no substantial change in YS and UTS values in different sample directions indicating the presence of low in- plane anisotropy (Fig. 5c). On the other hand, the elongation is least along longitudinal direction and maximum along 45° (Fig. 5c and Table 1). Differential curves of the experimental alloy exhibit similar nature in all the three sample directions (Fig. 5d). This shows that the work hardening rate ($d\sigma/d\varepsilon_p$) drops rapidly up to 0.4% strain and then gradually decreases up to 0.6%. It becomes nearly constant for further deformation.

The log true stress vs. log true strain curves are shown in Fig. 5e, which display two slopes. The flow curves having two slopes as observed in present study (Fig. 5e) have been reported in austenite stainless steel and other FCC materials with low stacking fault energy [23]. Such a two-slope behavior has been attributed to two deformation mechanisms. First relates to planar flow of dislocations during initial deformation. The second pertains to cross-slip and consequent cell formation with increasing strain. Ludwigson has modified the Ludwik relation ($\sigma = K\varepsilon^n$) to describe the plastic flow of these materials [23]. The modified relation is $\sigma = K_1\varepsilon^{n_1} + e^{K_2}e^{n_2\varepsilon}$. The K_1 and n_1 have same meaning as K and n in the Ludwik relation whereas K_2 and n_2 are components of a term that describes the positive departure of flow curve from Ludwik relation at low strains. The flow curve parameters of the present alloy have been calculated using modified Ludwik relation and are given in Table 2. As mentioned above, two slopes observed in Fig. 5e clearly indicate the occurrence of two mechanisms during tensile test. The initial mechanism transforms to other mode at a particular strain level called transition strain (Table 2).

The two-slope flow behavior and associated deformation mechanisms, as mentioned above has been reported in single-phase materials [23]. As stated earlier, this investigation deals with Ti–16Nb alloy having of α″ phase and small amount of β. The origin of the two-slope behavior, therefore, needs to be understood on different footing. In this respect, information pertaining to stress induced β → α″ transformation [10,24] in β type Ti-based alloys may be helpful. It appears that the first stage of two-slope behavior can be understood in terms of (i) β → α″ transformation and (ii) deformation of prior α″ phase. After the transition strain, the sample displays flow behavior of α″ phase only. To substantiate our explanation, the XRD pattern of the sample after tensile test was recorded. The pattern clearly shows disappearance of (2 0 0) peak of β phase (see inset (b) in Fig. 3). The second slope thus corresponds to the overall deformation occurring simultaneously in primary and transformed orthorhombic martensitic (α″) phases. The transition strain is maximum along longitudinal direction and minimum along transverse direction. The presence of small amount of the β phase and associated β → α″ transformation is likely to affect the deformation of the α″ phase during tensile test. The sample direction dependence of transition strain can therefore, be attributed to orientation of α″ phase as well as the distribution of β phase in the hot rolled specimen.

The yield locus of the experimental alloy is shown in Fig. 6. A best-fit ellipse drawn from all the six points does indicate the presence of anisotropy since all the experimental points do not lie on ellipse. The extent of anisotropy is rather small which can be seen from the sum of the root mean square distances between experimental points and yield locus (0.01×10^7). The yield strengths in tension and compression calculated from yield locus plot along longitudinal (σ_x) and transverse (σ_y) directions are given in Table 1. This further confirms the presence of low in-plane anisotropy in the hot rolled material. This observation is in agreement with the in-plane anisotropy obtained by the tensile test (Table 1).

It is evident from Table 1 that the yield strengths determined by Knoop hardness appear to be 5–6 times higher than that of those obtained by tensile tests. Such a difference is due to the fact that the exact quantitative determination of the yield strength by the

Table 2
Flow curve parameters of the hot rolled Ti–16Nb alloy.

Sample	K_1 (MPa)	n_1	K_2 (MPa)	$-n_2$	Transition strain	Error[a]
Longitudinal (L)	1017	0.092	4.28	97.10	1.46	.008
45°	1121	0.140	5.06	56.64	1.33	.030
Transverse (T)	1064	0.118	5.05	57.57	1.26	.030

[a] The error has been calculated by considering root mean square deviation between experimental and calculated σ values.

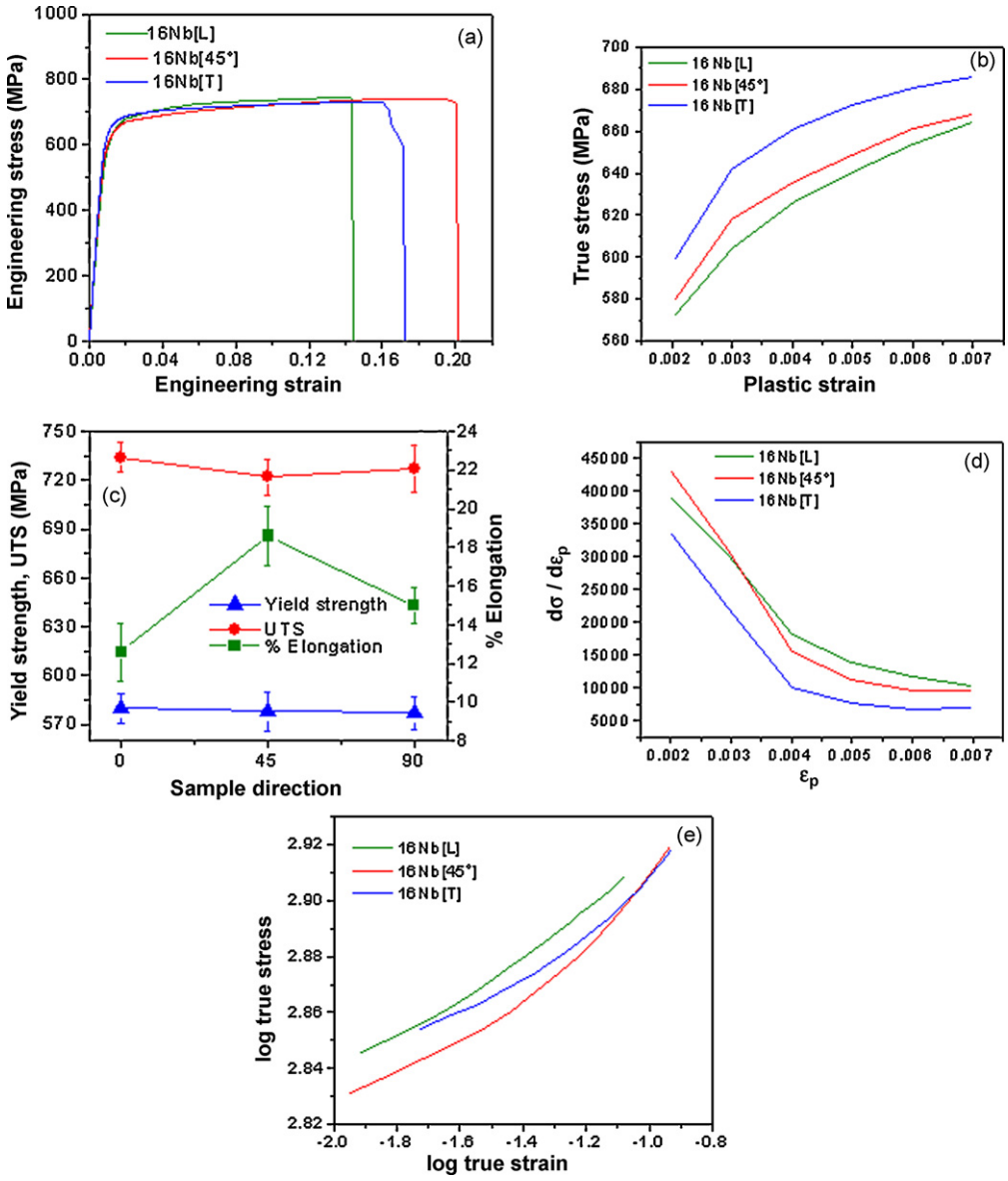

Fig. 5. Tensile properties of the hot rolled Ti–16Nb alloy: (a) Engineering stress–engineering strain curves up to fracture, (b) True stress–true strain curves, (c) Variation of YS, UTS and elongation with sample direction, (d) differential curves and (e) log true stress–log true strain curves.

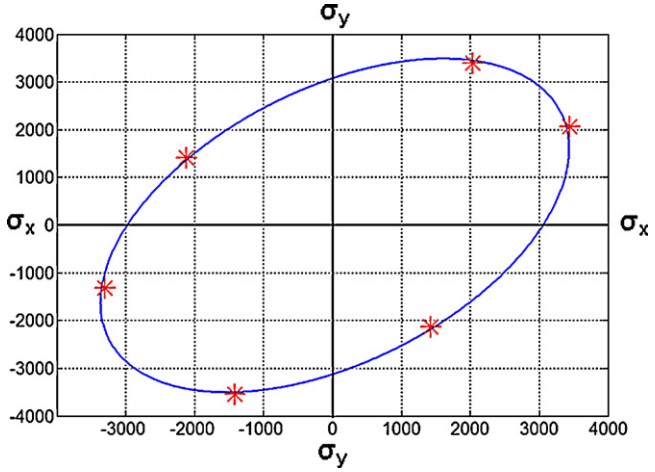

Fig. 6. Yield locus plot of the hot rolled experimental alloy.

Knoop hardness method is not possible. This method can be used only to the extent that they are a measure of relative indentation of the resistance of a material to the specific condition of deformation [25]. It is also necessary to identify the role of friction and the degree of localized deformation under the indenter so that the true nature of measurement can be evaluated. In literature, the yield locus plots are calibrated with tensile data obtained from the longitudinal and transverse directions. However, yield stresses are usually measured in a uniaxial tension/compression tests, which do not constrain the flow pattern during deformation. As a result, such a test does not model the situation under an indenter, where complex and highly constrained flow patterns exist.

Low in-plane anisotropy in hot rolled titanium alloys has been attributed to development of basal texture in α (cph) phase [3,6,7]. The anisotropy of hot rolled materials can be calculated by % in-plane anisotropy, which is defined as [26]

$$\%\mathrm{IPA} = \left[\frac{\{2\mathrm{YS(L)} - \mathrm{YS(T)} - \mathrm{YS}(45^\circ)\}}{2\mathrm{YS(L)}}\right] \times 100$$

The present alloy mainly consists of the α″ phase, which exhibits low % in-plane anisotropy (0.34%). The (0 0 2) pole figure of the α″ phase consists of basal component corresponding to [0 0 1]||ND fiber and other fiber located in between $\Phi = 58$ and 68°. The (0 2 0) and (1 1 1) pole figures also display the presence of fibers. The low in-plane anisotropy both in terms of YS, UTS and yield locus observed in the present study can be attributed to these fibers. It appears that the hot rolled Ti–16Nb alloy has good capability for forming processing due to low in-plane anisotropy with reasonably high ductility.

4. Summary

A correlation amongst texture, in-plane anisotropy in tensile properties and yield locus has been established. It has been shown that work hardening curves of the alloy in three different sample directions exhibit two slopes indicating the occurrence of two different mechanisms during tensile test and follow the modified Ludwik equation.

Acknowledgments

The authors are grateful to Ministry of Defence, Government of India for financial support and Director, DMRL, Hyderabad for constant encouragement. We extend our thanks to Dr. M. Srinivas, Dr. S.V. Kamat and Dr. T. K. Nandy for many fruitful discussions.

References

[1] A.K. Singh, R.A. Schwarzer, Z. Metallkd. 91 (2000) 702.
[2] A.K. Singh, R.A. Schwarzer, Trans. IIM 61 (2008) 371.
[3] Z. Yongqing, L. Zuochen, L. Changliang, W. Qingzhi, in: Z. Liang, L. Zho, Y. Chen (Eds.), Texture of Materials (ICOTOM-10), Proceedings of the eleventh International Conference on Texture of Materials, Academic Publishers, Xiang, Beijing, China, 1996, p. p909.
[4] M.F. Amateau, D.L. Dull, L. Raymond, Metall. Trans. 5 (1974) 561.
[5] C. Muller, A. Gysler, G. Luetjering, in: P. Lacombe, R. Tricot, G. Beranger (Eds.), Proceedings of Sixth World Conference on Titanium, Cedex, France, 1988, p. p351.
[6] M.J. Phillippe, F. Wagner, C. Esling, in: J.S. Kallend, G. Gottstein (Eds.), Eight International Conference on Textures of Materials (ICOTOM-8), The Metallurgical Society, Pennsylvania, 1988, p. p837.
[7] M.J. Phillippe, C. Esling, B. Hocheid, Textures and Microstructures 7 (1988) 265.
[8] M.J. Phillippe, F.E. Mellab, F. Wagner, C. Esling, B. Hocheid, in: P. Lacombe, R. Tricot, G. Beranger (Eds.), Proceedings of Sixth World Conference on Titanium, Cedex, France, 1988, p. p135.
[9] Z.S. Zhu, R.Y. Liu, M.G. Yan, C.X. Cao, J.L. Gu, N.P. Chen, J. Mater. Sci. 32 (1997) 5163.
[10] T.W. Durig, J. Albrecht, D. Richter, P. Fischer, Acta Metall. 30 (1982) 2161.
[11] M. Young, E. Levine, H. Margolin, Metall. Trans. 5A (1974) 1891.
[12] Y. Mantani, M. Tajima, Mater. Sci. Eng. A438–A440 (2006) 315.
[13] E.W. Collings, Physical Metallurgy of Titanium Alloys, American Society of Metals, Materials Park, Columbus, OH, 1948.
[14] U. Zwiker, K. Buhler, R. Muller, in: H. Kimura, O. Izumi (Eds.), Titanium 80 – Science and Technology, AIME, NY, 1980, p. 505.
[15] Y.H. Kim, J.Y. Wang, Y.N. Pan, Mater. Trans. 44 (2003) 2384.
[16] M. Niinomi, Metall. Mater. Trans. 33A (2002) 477.
[17] C.Y. Cui, D.H. Ping, J. Alloys Compd. 471 (2009) 248.
[18] R.G. Wheeler, D.R. Ireland, Electrochem. Technol. 4 (1966) 313.
[19] D. Lee, W.A. Backofen, Trans. AIME 236 (1966) 1696.
[20] L.G. Schultz, J. Appl. Phys. 20 (1949) 1039.
[21] H.J. Bunge, Texture Analysis in Materials Science, Butterworth, London, 1982.
[22] N. Stefanson, I. Weiss, A.J. Hutt, P.G. Allen, P.J. Bania, Titanium 95, science and technology, in: P.A. Blenkinsop, W.J. Evans, H.M. Flower (Eds.), Proceedings of the Eighth world conference on Titanium, Birmingham, UK, 1995, p. p980.
[23] D.C. Ludwigson, Metall. Trans. 2 (1971) 2825.
[24] D.H. Ping, C.Y. Cui, F.X. Yin, Y. Yamaka-Mitari, Scripta Mater. 54 (2006) 1305.
[25] D. Lee, in: J.H. Westbrook, H. Conrad (Eds.), Science of Hardness Testing and Its Research Applications, ASM International, Metals Park, Ohio, 1973, p. p147.
[26] K.V. Jata, A.K. Hopkins, R.J. Rioja, Mater. Sci. Forum 217–222 (1996) 647.